American Mineralogist, Volume 69, pages 307–318, 1984

Heat capacity and thermodynamic functions for gehlenite and staurolite: with comments on the Schottky anomaly in the heat capacity of staurolite

BRUCE S. HEMINGWAY AND RICHARD A. ROBIE

U.S. Geological Survey
Reston, Virginia 22092

Abstract

The heat capacities of a synthetic gehlenite and a natural staurolite have been measured from 12 and 5 K, respectively, to 370 K by adiabatic calorimetry, and the heat capacities of staurolite have been measured to 900 K by differential scanning calorimetry. Staurolite exhibits a Schottky thermal anomaly having a maximum near 21 K.

Smoothed values of the thermodynamic properties of heat capacity, entropy, and enthalpy function and Gibbs energy function are given for integral temperatures. The entropy of gehlenite, $Ca_2Al_2SiO_7$, at 298.15 K and 1 bar is 210.1±0.6 J/(mol · K), which includes a configurational contribution of 11.506 J/(mol · K). The entropy of staurolite at 298.15 K and 1 bar is reported for two compositions as 1019.6±12.0 J/(mol · K) for $H_2Al_2Fe_4Al_{16}Si_8O_{48}$ and 1101.0±12.0 J/(mol · K) for $(H_3Al_{1.15}Fe^{2+}_{0.60})(Fe^{2+}_{2.07}Fe^{3+}_{0.54}Ti_{0.08}Mn_{0.02}Al_{1.19})(Mg_{0.44}Al_{15.26})Si_8O_{48}$ where the configurational entropy contributions are 34.6 and 121.0 J (mol · K), respectively. In addition, the entropy value reported for the second staurolite composition contains an additional 10 J representing the estimated contribution of the magnetic entropy below about 5 K.

Introduction

The heat capacities of gehlenite were measured between 12 and 380 K in this study in order to reduce the uncertainty associated with the rather large extrapolation necessary to obtain the entropy contribution below 50 K from the older heat capacity data that were measured between 50 and 298 K by Weller and Kelley (1963). High-temperature heat-content data for gehlenite were reported by Pankratz and Kelley (1964).

The heat capacities of staurolite were measured in this study between 5 and 368 K by low-temperature adiabatic calorimetry and between 340 and 900 K by differential scanning calorimetry. We are not aware of previous heat-capacity measurements for staurolite. The single set of heat-capacity results has been corrected to two staurolite compositions, and estimates of the Schottky heat capacity have been made upon the basis of several simple models for determining the lattice heat capacity for staurolite. Similarly, simple models have been used to estimate configurational entropy terms for each staurolite formulation.

Materials

The gehlenite sample was a portion of the sample used by Woodhead (1977). A complete description of the sample preparation and of the physical and chemical properties of the sample was given by Woodhead. The sample was designated 75001H by Woodhead. The gehlenite was annealed at 1525°C for 20 hours from a glass of gehlenite composition. The annealed sample was crushed and material less than 150 mesh was removed. The sample mass was 28.0825 g. The cell parameters were a = 7.68658(23)Å and c = 5.06747(11)Å and the calculated cell volume was 9.01559(51) J/bar (Woodhead, 1977, Table 3-3). Woodhead also reported that 10% of the glass remained after the 20 hours of annealing.

The chemical and physical properties of the staurolite sample were described by Zen (1981, Table 4, page 124, sample 355-1). The sample represented a separate of natural staurolite from the Everett Formation collected near Lions Head, Conn. The crushed sample was dry sieved to remove material smaller than 150 mesh. The sample mass was 31.9650 g for the low-temperature calorimetric measurements and 39.900 mg for the differential scanning calorimetric measurements.

Experimental results

The low-temperature adiabatic calorimeter and the methods and procedures followed in this study are described elsewhere (Robie and Hemingway, 1972; Robie et al., 1976 and 1978). The heat capacities of staurolite were measured from 340 to 900 K by using a differential scanning calorimeter and following the procedures outlined by Krupka et al. (1979) and Hemingway et al. (1981). The onset of decomposition of this natural staurolite sample was 910±10 K, at a heating rate of 10 K/min.

0003–004X/84/0304–0307$02.00

The experimental specific heats for gehlenite and staurolite are given in Tables 1 and 2, respectively, in the chronological order of the measurements. The data have been corrected for curvature (Robie and Hemingway, 1972) but are uncorrected for chemical impurities.

Thermodynamic properties of gehlenite and staurolite

The measured specific heat data were graphically extrapolated to 0 K from a plot of C_p°/T *vs.* T^2. A more complete description of the treatment of the low-temperature data for staurolite is given in a subsequent section.

Smoothed values of the thermodynamic functions of heat capacity, C_p°; entropy, S_T°, or entropy increment, $S_T^\circ - S_0^\circ$; enthalpy function, $(H_T^\circ - H_r^\circ)/T$; and Gibbs energy function, $(G_T^\circ - H_r^\circ)/T$; where r is the reference temperature, are given in Tables 3 through 7 for gehlenite and for two compositions of staurolite as $(H_3Al_{1.15}Fe^{2+}_{0.60})(Fe^{2+}_{2.07}Fe^{3+}_{0.54}Ti_{0.08}Mn_{0.02}Al_{1.19})(Mg_{0.44}Al_{15.26})Si_8O_{48}$ and as $H_2Al_2Fe_4Al_{16}Si_8O_{48}$. The reference temperature for the low-temperature heat capacity data is 0 K whereas 298.15 K is used in the high-temperature tabulation.

Table 1. Experimental specific heats for synthetic gehlenite

Temp. K	Specific heat J/(g·K)	Temp. K	Specific heat J/(g·K)	Temp. K	Specific heat J/(g·K)
Series 1		Series 3		Series 7	
12.16	0.001579	98.01	0.2823	241.63	0.6583
13.41	0.002245	103.11	0.3009	247.11	0.6706
14.68	0.003088	108.10	0.3180	252.65	0.6803
16.07	0.004217	113.26	0.3357	258.32	0.6903
17.68	0.005851	118.59	0.3541	264.09	0.7001
19.63	0.008314			269.81	0.7092
21.60	0.01121	Series 4		275.47	0.7186
23.64	0.01477			281.20	0.7276
26.10	0.01943	110.43	0.3244	286.97	0.7356
29.03	0.02569	115.64	0.3422	292.82	0.7452
32.32	0.03408	120.65	0.3591	298.73	0.7538
35.85	0.04418	125.58	0.3749		
39.74	0.05638			Series 8	
44.16	0.07127	Series 5			
49.05	0.08866			296.20	0.7503
54.23	0.1088	135.90	0.4075	302.13	0.7587
		141.13	0.4230	308.00	0.7671
Series 2		146.32	0.4382	313.75	0.7741
		151.43	0.4528		
53.07	0.1044	156.46	0.4665	Series 9	
57.59	0.1222	161.49	0.4801		
62.54	0.1418	166.67	0.4937	310.62	0.7716
67.75	0.1625	172.13	0.5078	317.32	0.7801
72.73	0.1828	177.72	0.5220	323.97	0.7893
77.25	0.2012	183.20	0.5352	330.57	0.7977
81.85	0.2197			337.13	0.8062
86.91	0.2396	Series 6		343.65	0.8136
92.30	0.2607			350.12	0.8210
		180.54	0.5312	356.57	0.8282
		185.99	0.5441	363.26	0.8356
		191.27	0.5559	370.18	0.8435
		196.55	0.5681	377.07	0.8503
		201.90	0.5802	383.93	0.8556
		207.33	0.5921		
		212.84	0.6039		
		218.26	0.6154		
		223.64	0.6264		
		228.94	0.6367		
		234.20	0.6469		
		239.41	0.6573		

Table 2. Experimental specific heats for staurolite. Series 8 and 9 were results obtained by differential scanning calorimetry

Temp. K	Specific heat J/(g·K)	Temp. K	Specific heat J/(g·K)	Temp. K	Specific heat J/(g·K)
Series 1		Series 5		Series 9	
298.82	0.7635	104.13	0.1902	450.0	0.9674
304.85	0.7752	109.73	0.2098	460.0	0.9791
311.75	0.7877	115.37	0.2297	469.9	0.9853
319.09	0.8007	121.13	0.2507	479.9	0.9951
326.35	0.8131	126.92	0.2715	489.9	1.0051
		132.67	0.2924	499.9	1.0137
Series 2		138.38	0.3131	469.9	0.9843
		144.07	0.3335	479.8	0.9901
333.47	0.8253	149.75	0.3537	489.8	0.9960
340.62	0.8366	155.40	0.3735	499.8	1.0027
347.72	0.8473	161.03	0.3932	509.8	1.0076
354.75	0.8580	166.66	0.4125	519.8	1.0123
361.73	0.8679			529.8	1.0188
368.66	0.8779	Series 6		539.8	1.0262
				549.8	1.0321
Series 3		172.37	0.4317	559.8	1.0393
		178.03	0.4509	569.8	1.0478
4.80	0.003254	183.76	0.4695	579.8	1.0518
5.16	0.003375	189.46	0.4878	589.7	1.0596
5.68	0.003931	195.21	0.5056	599.7	1.0649
6.51	0.004568	200.95	0.5232	609.7	1.0713
7.57	0.005343	206.71	0.5397	619.7	1.0797
8.58	0.006177	212.54	0.5575	629.7	1.0876
9.47	0.006905	218.42	0.5741	639.7	1.0998
10.38	0.007708	224.47	0.5909	649.7	1.1125
11.35	0.008444	230.67	0.6076	619.8	1.0920
12.49	0.009165	237.09	0.6249	629.8	1.0990
13.83	0.009927	243.56	0.6417	639.7	1.1013
15.31	0.01071			649.7	1.1066
16.97	0.01145	Series 7		659.7	1.1120
18.82	0.01220			669.7	1.1174
20.86	0.01298	249.14	0.6551	679.7	1.1221
23.06	0.01375	255.51	0.6709	689.7	1.1262
25.46	0.01468	261.88	0.6857	699.7	1.1278
27.83	0.01577	268.32	0.7001	709.7	1.1338
30.19	0.01717	274.88	0.7146	719.7	1.1398
32.96	0.01922	281.56	0.7290	729.7	1.1425
36.44	0.02236	288.29	0.7433	739.7	1.1477
40.50	0.02676	295.21	0.7570	749.7	1.1510
44.97	0.03251	302.06	0.7699	759.7	1.1493
50.07	0.04051			789.7	1.1655
55.82	0.05141	Series 8		779.7	1.1640
				789.7	1.1705
Series 4		340.10	0.8397	799.7	1.1802
		350.10	0.8550	849.4	1.1678
55.82	0.05170	360.10	0.8690	898.9	1.1961
61.41	0.06333	370.10	0.8794		
66.88	0.07595	380.10	0.8921		
73.02	0.09191	390.10	0.9061		
79.11	0.1093	400.00	0.9154		
84.95	0.1270	410.00	0.9289		
90.76	0.1455	420.00	0.9394		
96.35	0.1638	430.00	0.9447		
101.90	0.1826	440.00	0.9578		

Following Ulbrich and Waldbaum (1976), a zero point entropy, S_0°, contribution of 11.506 J/(mol · K) is included in the Gibbs energy function for gehlenite in Table 3. The entropy of gehlenite at 298.15 K and 1 bar, is, therefore, 210.1±0.6 J/(mol · K). The values for the Gibbs energy function tabulated for the two staurolite compositions do not include a zero point entropy contribution. This contribution is discussed, at length, below.

It should be noted that Woodhead (1977) has considered the question of how disorder in Si/Al on the T_2 site would be reflected in the crystal structure of gehlenite. Woodhead concluded that gehlenite forming at low temperatures would obey the aluminum avoidance rule for

Table 3. Molar thermodynamic properties of gehlenite, $Ca_2Al_2SiO_7$.

TEMP.	HEAT CAPACITY	ENTROPY	ENTHALPY FUNCTION	GIBBS ENERGY FUNCTION
T	C_P°	$(S_T^\circ-S_0^\circ)$	$(H_T^\circ-H_0^\circ)/T$	$-(G_T^\circ-H_0^\circ)/T$
KELVIN		J/(mol·K)		
5	.0306	.0104	.0075	11.506
10	.239	.0785	.0583	11.526
15	.914	.279	.211	11.566
20	2.421	.725	.555	11.676
25	4.742	1.501	1.147	11.856
30	7.690	2.613	1.980	12.136
35	11.44	4.075	3.059	12.522
40	15.69	5.875	4.367	13.014
45	20.36	7.989	5.881	13.614
50	25.37	10.39	7.577	14.320
60	36.04	15.95	11.42	16.03
70	47.15	22.34	15.73	18.11
80	58.25	29.36	20.35	20.51
90	69.01	36.85	25.17	23.19
100	79.25	44.65	30.07	26.09
110	88.91	52.66	34.98	29.19
120	98.04	60.80	39.86	32.44
130	106.7	68.99	44.67	35.82
140	115.0	77.20	49.40	39.31
150	123.0	85.41	54.04	42.87
160	130.6	93.59	58.59	46.51
170	137.9	101.7	63.04	50.19
180	144.9	109.8	67.40	53.92
190	151.6	117.8	71.65	57.68
200	157.9	125.8	75.81	61.46
210	164.0	133.6	79.86	65.26
220	169.7	141.4	83.82	69.06
230	175.1	149.0	87.67	72.87
240	180.3	156.6	91.42	76.69
250	185.2	164.1	95.08	80.49
260	190.0	171.4	98.64	84.29
270	194.6	178.7	102.1	88.08
280	199.0	185.8	105.5	91.85
290	203.2	192.9	108.8	95.61
300	207.2	199.8	112.0	99.36
310	211.1	206.7	115.1	103.1
320	214.9	213.5	118.2	106.8
330	218.6	220.1	121.2	110.5
340	222.0	226.7	124.1	114.1
350	225.1	233.2	126.9	117.8
360	228.1	239.6	129.7	121.4
370	231.2	245.9	132.4	125.0
380	233.8	252.1	135.0	128.5
273.15	196.0	180.9	103.2	89.27
298.15	206.5	198.6	111.4	98.66

the T_2 sites. Following the interpretation given by Woodhead, the configurational entropy for gehlenite would be 5.75J(mol · K). Gehlenites synthesized at higher temperatures appear to have greater disorder leading Woodhead to conclude that disorder of Si/Al on the T_2 site would be temperature dependent.

The heat capacities for gehlenite were not corrected for the 10% of uncrystallized glass (Woodhead, 1977). Robie et al. (1978) have shown that the heat capacities of the feldspars analbite, high sanidine, and anorthite differ little from the heat capacities of glasses of the same composition. These observed differences yielded calculated differences of 0.8 to 2.3% in $S_T - S_0$. We can assume (as a first approximation) that the difference in the gehlenite system should be no larger than that in the feldspar system. Consequently, the uncertainty in the functions $S_T - S_0$ and $(H_T - H_0)/T$ should be 0.2% or less, which is within the experimental uncertainty of the data.

The measured heat capacities of natural staurolite were corrected to the two compositions listed above by assuming the principle of additivity and representing the sample as, first, for Tables 4 and 6, 1665.140 g of staurolite, 4.282 g of corundum, 1.514 g of lime, 4.394 g of zincite, 0.503 g of FeO, 0.403 g of periclase, 0.479 g of rutile, 0.426 g of P_2O_5, 0.468 g of ice, and a deficiency of 0.142 g of manganosite, and second, for Tables 5 and 7, 1703.737 g of staurolite, 356.263 g of pyrophyllite, 17.029 g of brucite, 73.399 g of magnesioferrite, 5.430 g of hematite, 328.725 g of corundum, 2.243 g of lime, 10.227 g of rutile, 0.710 g of P_2O_5, 1.986 g of manganosite, and 6.510 g of zincite. The corrections represent a change in the specific

Table 4. Low-temperature molar thermodynamic properties of staurolite, $(H_3Al_{1.15}Fe^{2+}_{0.60})(Fe^{2+}_{2.07}Fe^{3+}_{0.54}Ti_{0.08}Mn_{0.02}Al_{1.19})(Mg_{0.44}Al_{15.26})Si_8O_{48}$. The data are uncorrected for chemical site-configurational contributions to the entropy.

TEMP.	HEAT CAPACITY	ENTROPY	ENTHALPY FUNCTION	GIBBS ENERGY FUNCTION
T	C_P°	$(S_T^\circ-S_0^\circ)$	$(H_T^\circ-H_0^\circ)/T$	$-(G_T^\circ-H_0^\circ)/T$
KELVIN		J/(mol·K)		
5	5.37	2.99	2.08	0.91
10	12.32	8.87	5.47	3.40
15	17.55	14.95	8.71	6.24
20	21.04	20.50	11.38	9.12
25	24.03	25.51	13.61	11.90
30	28.19	30.23	15.66	14.57
35	34.54	35.04	17.89	17.15
40	43.06	40.18	20.47	19.70
45	53.98	45.86	23.57	22.29
50	67.16	52.21	27.25	24.96
60	99.69	67.21	36.50	30.70
70	139.5	85.48	48.29	37.18
80	185.8	107.1	62.53	44.54
90	237.3	131.9	79.04	52.83
100	292.6	159.7	97.60	62.11
110	350.6	190.3	118.0	72.35
120	410.0	223.4	139.8	83.54
130	470.2	258.5	162.9	95.64
140	530.3	295.6	187.0	108.6
150	590.0	334.2	211.9	122.3
160	648.6	374.2	237.4	136.8
170	705.8	415.2	263.2	152.0
180	761.1	457.1	289.4	167.8
190	814.5	499.7	315.6	184.1
200	866.0	542.8	341.9	201.0
210	915.6	586.3	368.0	218.3
220	963.4	630.0	394.0	236.0
230	1009.2	673.8	419.7	254.1
240	1053.0	717.7	445.2	272.5
250	1094.8	761.6	470.4	291.2
260	1134.7	805.3	495.2	310.1
270	1172.7	848.8	519.6	329.3
280	1208.9	892.1	543.5	348.6
290	1243.3	935.2	567.1	368.1
300	1276.0	977.9	590.2	387.7
310	1306.9	1020.2	612.8	407.4
320	1336.5	1062.2	635.0	427.2
330	1365.0	1103.7	656.6	447.1
340	1392.2	1144.9	677.9	467.0
350	1417.7	1185.6	698.7	487.0
360	1442.0	1225.9	719.0	506.9
365	1454.0	1245.9	729.0	516.9
273.15	1184.3	862.5	527.2	335.3
298.15	1270.1	970.0	585.9	384.0

Table 5. Low-temperature molar thermodynamic properties of staurolite, $H_2Al_2Fe_4Al_{16}Si_8O_{48}$. The data are uncorrected for chemical site-configurational contributions to the entropy.

TEMP.	HEAT CAPACITY	ENTROPY	ENTHALPY FUNCTION	GIBBS ENERGY FUNCTION
T	C_P°	$(S_T^\circ-S_0^\circ)$	$(H_T^\circ-H_0^\circ)/T$	$-(G_T^\circ-H_0^\circ)/T$
KELVIN		J/(mol·K)		
5	3.38	4.07	2.97	1.10
10	18.28	12.97	8.19	4.78
15	25.38	21.88	12.87	9.01
20	29.08	29.75	16.51	13.24
25	31.47	36.51	19.28	17.23
30	34.71	42.49	21.54	20.95
35	40.08	48.23	23.79	24.44
40	47.67	54.05	26.28	27.77
45	57.73	60.22	29.19	31.03
50	70.12	66.92	32.65	34.28
60	101.1	82.33	41.36	40.96
70	139.5	100.7	52.55	48.15
80	184.6	122.2	66.18	56.03
90	235.4	146.8	82.11	64.72
100	290.4	174.4	100.2	74.29
110	348.2	204.8	120.1	84.76
120	407.5	237.6	141.5	96.11
130	467.7	272.6	164.3	108.3
140	528.0	309.5	188.1	121.4
150	587.9	348.0	212.8	135.2
160	647.0	387.8	238.1	149.7
170	704.6	428.8	263.8	164.9
180	760.5	470.6	289.9	180.8
190	814.4	513.2	316.1	197.1
200	866.5	556.3	342.3	214.0
210	916.9	599.8	368.5	231.3
220	965.4	643.6	394.5	249.1
230	1012.0	687.6	420.4	267.2
240	1056.6	731.6	445.9	285.6
250	1099.0	775.6	471.2	304.3
260	1139.5	819.5	496.2	323.3
270	1178.1	863.2	520.7	342.5
280	1214.9	906.7	544.8	361.9
290	1249.9	950.0	568.6	381.4
300	1283.1	992.9	591.8	401.1
310	1314.5	1035.5	614.6	420.9
320	1344.6	1077.7	637.0	440.7
330	1373.7	1119.5	658.9	460.7
340	1401.6	1161.0	680.3	480.6
350	1427.7	1202.0	701.3	500.7
360	1452.3	1242.5	721.8	520.7
365	1464.7	1262.7	731.9	530.7
273.15	1139.9	876.9	528.4	348.6
298.15	1277.1	985.0	587.6	397.4

heat (J/g · K, the quantity actually measured) of less than 0.1% for the first case given above for heat-capacity values above 125 K and of less than 1% for values from 8 to 125 K, and for the second composition, of less than 1% above 300 K, less than 2% from 150 to 300 K, and less than 3% from 50 to 150 K. Below 50 K, the sum of the specific heats of the impurity phases becomes negligible compared to the measured specific heat of staurolite.

It is both instructive and important to examine the assumptions and procedures underlying the corrections applied to the specific-heat data, particularly in light of the rather large mass correction necessary to obtain the heat capacities of staurolite as listed in Tables 5 and 7. Samples are initially chosen on the basis of chemical purity and/or approximately correct stoichiometry. Corrections for small deviations from ideality are made assuming that the impurities can be represented by phases for which specific heat data are available. Most geochemists believe that ideal additivity does not truly prevail, but where the required corrections are small (i.e., where the impurities represent only a small percentage of the sample) the error associated with the correction is often less than the uncertainty in the measured specific heat.

The potential errors associated with this type of correction may be minimized by combining the impurity components into phases that are structurally similar to the phase under study (Robie et al., 1976 and Klotz, 1950), or by using a corresponding states argument (Robie et al., 1982, or Stout and Catalano, 1955). In either case, the corrections may be applied directly to the measured specific heats (Robie et al., 1976) in order to provide corrected thermodynamic parameters as a function of temperature, or the integrated properties may be corrected at a specific temperature (Westrum et al., 1979). Both procedures should yield the same results at the same temperature if the same components are chosen.

Two models are presented in Table 8 in which the heat capacities of staurolite as given in Tables 4 and 6 are approximated by the summation approach. In model 1, the heat capacity of staurolite is approximated by the summation of the heat capacities of equivalent oxide

Table 6. High-temperature molar thermodynamic properties for natural staurolite. The formula for staurolite is given in Table 4. A chemical site-configurational entropy of 121.0 J/(mol · K) and an additional 10.0 J/(mol · K) of magnetic entropy have been added to the entropy at 298.15 K given in Table 4. The equation fit the experimental data with an average deviation of 0.5%.

TEMP.	HEAT CAPACITY	ENTROPY	ENTHALPY FUNCTION	GIBBS ENERGY FUNCTION
T	C_P°	S_T°	$(H_T^\circ-H_{298}^\circ)/T$	$-(G_T^\circ-H_{298}^\circ)/T$
KELVIN		J/(mol·K)		
298.15	1270.1	1101.0	0.0	1101.0
325	1349.2	1214.0	108.3	1105.7
350	1413.0	1316.3	199.2	1117.1
375	1469.4	1415.8	282.1	1133.7
400	1519.7	1512.3	357.9	1154.4
425	1564.9	1605.8	427.6	1178.2
450	1605.8	1696.4	491.9	1204.5
475	1643.1	1784.2	551.5	1232.7
500	1677.4	1869.4	607.0	1262.4
525	1708.9	1952.0	658.7	1293.3
550	1738.1	2032.2	707.1	1325.1
575	1765.3	2110.1	752.6	1357.5
600	1790.6	2185.7	795.3	1390.4
625	1814.3	2259.3	835.6	1423.7
650	1836.6	2330.9	873.7	1457.3
675	1857.5	2400.6	909.7	1490.9
700	1877.2	2468.5	943.9	1524.6
725	1895.9	2534.7	976.4	1558.3
750	1913.6	2599.3	1007.4	1591.9
775	1930.3	2662.3	1036.9	1625.5
800	1946.2	2723.9	1065.0	1658.8
825	1961.3	2784.0	1092.0	1692.0
850	1975.6	2842.7	1117.8	1725.0
875	1989.3	2900.2	1142.5	1757.8
900	2002.4	2956.4	1166.2	1790.3

Table 7. High-temperature molar thermodynamic properties for ideal staurolite, $H_2Al_2Fe_4Al_{16}Si_8O_{48}$. A chemical site-configurational entropy of 34.6 J/(mol · K) has been added to the entropy at 298.15 K given in Table 5. The equation fit the experimental data with an average deviation of 0.8%.

TEMP.	HEAT CAPACITY	ENTROPY	ENTHALPY FUNCTION	GIBBS ENERGY FUNCTION
T	C_P°	S_T°	$(H_T^\circ - H_{298}^\circ)/T$	$-(G_T^\circ - H_{298}^\circ)/T$
KELVIN		J/(mol·K)		
298.15	1277.1	1019.6	0.0	1019.6
325	1357.4	1133.2	108.9	1024.3
350	1422.3	1236.2	200.5	1035.8
375	1479.6	1336.4	283.9	1052.5
400	1530.7	1433.5	360.2	1073.3
425	1576.8	1527.7	430.5	1097.3
450	1618.5	1619.0	495.3	1123.7
475	1656.6	1707.6	555.4	1152.1
500	1691.6	1793.5	611.4	1182.1
525	1723.9	1876.8	663.6	1213.2
550	1753.9	1957.7	712.5	1245.2
575	1781.9	2036.3	758.4	1277.9
600	1808.0	2112.7	801.6	1311.1
625	1832.6	2187.0	842.3	1344.6
650	1855.7	2259.3	880.9	1378.4
675	1877.6	2329.8	917.4	1412.4
700	1898.3	2398.4	952.0	1446.4
725	1917.9	2465.4	985.0	1480.4
750	1936.6	2530.7	1016.4	1514.3
775	1954.4	2594.5	1046.4	1548.1
800	1971.4	2656.8	1075.0	1581.8
825	1987.7	2717.7	1102.5	1615.3
850	2003.2	2777.3	1128.7	1648.6
875	2018.2	2835.6	1153.9	1681.7
900	2032.5	2892.6	1178.1	1714.5

components. Two major changes are presented in model 2. First, approximation of the contribution of OH to the specific heat of staurolite in model 1 is made by assuming that model 1 contains ice and water, whereas in model 2, the OH contribution is introduced through pyrophyllite and brucite. Second, the contribution of Fe^{2+} as FeO in model 1 was replaced through the introduction of the difference in the specific heat of a mixed Mg–Fe enstatite and the specific heat of pure Mg enstatite (Krupka et al., 1978, unpublished data), where this difference represented the composition $FeSiO_3$.

Differences were calculated by subtracting the summed values for each model from the smoothed heat capacities given in Tables 4 and 6. These differences are shown in Figure 1. At temperatures greater than 300 K, relatively little advantage is obtained by adopting one specific heat model over the other, with the exception of the effect of the $\alpha - \beta$ transition in quartz. The specific heat of a transition in an oxide component is usually removed by a smoothing process. For the model 1 data presented in Figure 1, the effect of the $\alpha - \beta$ transition has been preserved as a visual reminder that when using the integrated properties (e.g., entropy) approach, an additional correction may be required in order to maintain smooth estimated values.

Although local deviations of the model 2 specific heat data from the measured heat capacity of staurolite are relatively large at low temperatures, the entropy as $S_T -$

Table 8. Model 1 and 2 compositional approximations to natural staurolite.

Phase	Model 1	Model 2	Phase	Model 1	Model 2
	Moles			Moles	
SiO_2	8.00	----	TiO_2	0.08	0.08
Al_2O_3	8.80	7.47	MnO	0.02	0.02
FeO	2.67	----	H_2O	1.50	----
Fe_2O_3	0.268	0.268	Pyrophyllite	----	1.33
MgO	0.44	0.27	$FeSiO_3$	----	2.67
$Mg(OH)_2$	----	0.17			

S_0 of the model 2 data at 298.15 K differs by only +0.2%, whereas that of model 1 is nearly 8% greater. At 900 K, model 2 differs by −1% whereas model 1 differs by +6%. The values of $S_T - S_0$ have been corrected for the transitions in FeO, SiO_2, and H_2O. Consequently, the best overall fit is obtained from model 2.

The success of the model 2 components over those chosen for model 1 lies in the similarity of the magnetic

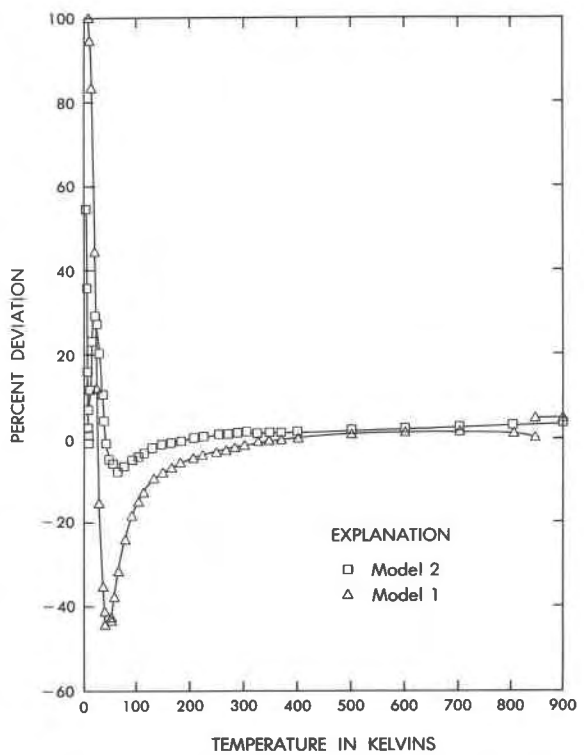

Fig. 1. The percentage deviation of the model 1 and 2 (see text) summations from the measured heat capacity of staurolite. Positive deviations indicate values of the models which are smaller than the observed heat capacity of staurolite.

contribution of Fe^{2+} in enstatite and staurolite. The cooperative ordering effect in FeO is of a different form than the apparent Schottky-type anomaly seen in the dilute paramagnetic salts, staurolite and enstatite; see Figure 2. In addition, pyrophyllite is a better approximation of the contribution of OH to the heat capacity of staurolite than the separate oxide components of corundum, quartz, and ice. The heat capacity data for the natural staurolite sample have been corrected to two arbitrarily chosen compositions as an example of the procedure. These corrections are only first approximations because we do not have sufficient data to estimate mixing properties. These results may be adjusted in a similar manner to estimate values for other staurolite compositions.

Magnetic entropy of staurolite

Schottky (1922) postulated that the electronic system of some atoms in a crystal would undergo excitation between a ground state and higher energy states. Each energy state is also characterized by a degree of degeneracy. For a simplified case in which there are two levels, each with equal degeneracy, it can be shown that the contribution to the heat capacity of a crystal arising from the presence of electrons in an excited energy level is equal to the difference between two Einstein models that are related by two characteristic frequencies f_E and $2f_E$ (see, for example, Gopal, 1966). Therefore, the contribution to the heat capacity and entropy of a material from the presence of excited energy states is related to the number of these energy levels and to their degeneracies.

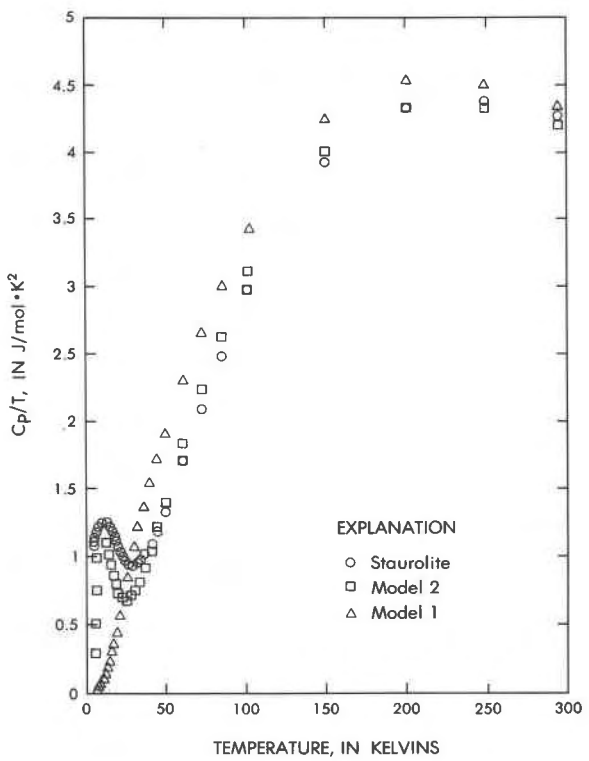

Fig. 2. A comparison of the heat capacity of staurolite and the values obtained from the model 1 and 2 summations (see text). The data are presented as C_p/T to emphasize the Schottky anomaly in staurolite.

The free ferrous ion has 25-fold degeneracy in the ground state that can be reduced or removed, when the ferrous ion is in a crystal, through the combined or separate effects of the local crystal field and cooperative spin-orbit coupling. The spatial distribution of the electronic charge of the free ion is spherically symmetrical. However, when the ion is placed in a crystal the spacial distribution of charges is altered by the distribution of charges in the neighboring atoms. Charge distributions (in the form of lobes and other shapes) that are directed toward other atoms are elevated to higher energy levels (splitting of levels) than those that are directed between neighboring atoms. Thus lower symmetry sites produce greater splitting of energy levels. The effect of the typical crystal field upon the ferrous ion is to elevate (remove) 10 levels beyond that which could be energetically accessible. The crystal field also exerts a torque upon the orbital momentum resulting in the orbital momentum not being constant in direction and when resolved in Cartesian coordinates to average to zero. This process is called quenching of the magnetic moment of the angular momentum.

In some crystal structures the interaction between the energy states of one atom are not independent of the energy states of similar neighboring atoms. In such systems, a mean energy is required to induce population of the different energy states and the associated anomaly (typically a λ peak) in the heat capacity is called a cooperative anomaly. Examples of cooperative anomalies of this type may be found in Robie et al. (1982, a,b) for antiferromagnetic ordering in fayalite, tephroite and cobalt olivine.

A noncooperative system exists if the excitation of the energy states of the atoms in the structure are independent of the energy levels in the similar neighboring atoms. Where no interdependence exists between the energy levels of similar neighboring atoms, the total energy contributed is equal to the sum of the energies of the independent levels and theoretical treatment of the system is greatly simplified.

The cooperative and noncooperative anomalies will be called Schottky anomalies and the anomalies in the entropy or heat capacity will be called Schottky contributions. The Schottky contribution is most easily defined where the energy separation of the different levels is small. In these cases, the contribution is observed at very low temperatures where the lattice heat capacity becomes either a Debye-like contribution or an essentially negligible contribution of the measured heat capacity. At low temperatures the noncooperative Schottky heat capacity anomaly is typically expressed as a bell-shaped peak that

is skewed toward higher temperatures. The temperature of the peak is related to the separation of the levels and the amplitude of the peak is related to the ratio of the degeneracies of the levels (e.g., Gopal, 1966). Examples of this type of heat capacity anomaly may be found in the results of Hill and Smith (1953). It is far more difficult to recognize Schottky contributions to the measured heat capacities where the energy levels have a large energetic separation and the contribution occurrences are at higher temperatures. This subject has been excellently discussed by Westrum (1983) and therefore will not be discussed further in this report.

The magnetic contribution to the heat capacity of a system may be composed of both a cooperative and a noncooperative contribution. Raquet and Friedberg (1972) concluded that the angular momentum of the ^5D ground state of the Fe^{2+} ion in $FeCl_2 \cdot 4H_2O$ was quenced and that the ground state of the five spin components was fully split by the combined effects of spin ordering (cooperative) and crystal field splitting (noncooperative).

Mössbauer spectra taken at 4.2 K have been interpreted by Dickson and Smith (1976), Regnard (1976), and Scorzelli et al. (1976) as indicating antiferromagnetic ordering in staurolite. Regnard found an ordering temperature of 6 ± 1 K, and Dickson and Smith obtained 7 ± 1 K for the ordering temperature. However, the heat-capacity values obtained in the temperature range of 5 to 8 in this study do not indicate the strong cooperative exchange that is characteristic of antiferromagnetic ordering.

Dickson and Smith (1976) have observed ordering attributable to antiferromagnetic ordering in $FeAl_2O_4$ in Mössbauer spectra obtained at temperatures below 8 K. Because of the temperature dependence of magnetic susceptibility data, Roth (1964) suggested that antiferromagnetic ordering developed in $FeAl_2O_4$ below 8 K, but he failed to detect an antiferromagnetic state in $FeAl_2O_4$ using neutron diffraction. Roth assumed that $FeAl_2O_4$ failed to show antiferromagnetic order in neutron diffraction because of a strong interaction between Fe^{2+} in tetrahedrally and octahedrally coordinated sites that destroyed long range order on the tetrahedral sites. Similarly, long range order in staurolite may not develop.

Lyon and Giauque (1949) and Hill and Smith (1953) measured the heat capacities of the dilute paramagnetic ferrous salts ferrous sulfate heptahydrate and ferrous ammonium sulfate hexahydrate, respectively. Neither ferrous compound showed an anomaly in the heat capacity that would be consistent with an interpretation of antiferromagnetic ordering at low temperatures, although two maxima were observed in the low-temperature heat capacities of each phase. These maxima were interpreted to be associated with a splitting of the ground state of the ferrous ion into two levels of equal degeneracy with a separation of 3 to 6.5 cm^{-1} that gave rise to the specific-heat anomalies at 2 to 4 K and a second group of three levels centered at 38 cm^{-1} or less for the anomalies observed in the 15 to 20 K region. Thus, the ferrous ions in staurolite may develop small separations of the ground state similar to those seen in the dilute ferrous salts.

Raquet and Friedberg (1972) measured the heat capacity of a ferrous salt ($FeCl_2 \cdot 4H_2O$) of greater ferrous concentration than those studied by Lyon and Giaugue (1949) and Hill and Smith (1953). Raquet and Friedberg observed a sharp λ-type peak consistent with low-temperature antiferromagnetic ordering. However, the exchange energy associated with the antiferromagnetic ordering was an order of magnitude smaller than the zero-field splitting of the ground state of Fe^{2+}, that is, the λ peak for the cooperative process was at a lower temperature than the noncooperative anomaly.

Our heat-capacity results do not extend to a low enough temperature to rule out a cooperative interaction in staurolite nor do they rule out a small separation of a lower doublet of the Fe^{2+} ion. Bearing in mind the limitations of theory discussed above and the ambiguity associated with the chemistry of our staurolite sample, we shall use several simple methods in an attempt to estimate that portion of the magnetic heat capacity and, consequently, entropy not defined by our measurement.

In the preceding section, an empirical case was presented in which the entropy of staurolite was shown to be adequately approximated by the summation of entropies of the model 2 components but not as favorably predicted by the summation of entropies of the model 1 components. In this section, we shall examine the theoretical aspects of the magnetic entropy of staurolite, using a modified version of model 2 to approximate the staurolite lattice contribution to the entropy.

Staurolite is a paramagnetic salt. The low symmetry of the several sites in which the Fe^{2+} ion may be found (Smith, 1968, and Takéuchi et al., 1972) and the low concentration of Fe within several of those sites (Takéuchi et al.) allow us to initially assume an ideal state for each Fe^{2+} ion in which the ion interacts only with its immediate crystal field and not with other Fe ions. The same assumption can be made for Fe^{3+} and Mn^{2+}.

The iron transition group paramagnetic salts yield experimental magneton values consistent with calculations assuming a quenched angular momentum. Consequently, the contribution of the electronic system of the iron transition group ions to the entropy is $R\ln(2S + 1)$, where S is the spin quantum number for which $S = 2$ for Fe^{2+} and $S = 5/2$ for Mn^{2+} and Fe^{3+} (e.g., see Kittel, 1976).

Several empirical approaches have been used to extract the magnetic contributions to the entropy and/or heat capacity (e.g., Lyon and Giauque, 1949; Osborne and Westrum, 1953; Stout and Catalano, 1955; and Friedberg et al., 1962). Osborne and Westrum assumed that the lattice heat capacity could be approximated by the heat capacity of an isomorphous diamagnetic phase containing a similar cation. Lyon and Giauque, and Stout and

Catalano using a similar approach, corrected the heat capacity of the isomorphous diamagnetic phase using a corresponding-states argument. Friedberg et al. assumed that the lattice heat capacity behaved like that of a Debye solid having $C_P \propto T^3$ and that the magnetic contribution above the Schottky anomaly should go to zero as T^{-2}. Friedberg et al. plotted $C_P T^2$ as a function of T^5 and fit the data with a straight line. The slope of this line represented the best estimate of the constant for the Debye lattice approximation.

The use of an isomorphous diamagnetic phase as a model for the lattice heat capacity of a paramagnetic phase can be theoretically justified only if we assume that the Einstein and Debye temperatures of the model differ little from those of the true lattice and we recall the additive properties of the Schottky anomaly given in the first paragraph of this section.

None of these procedures is directly applicable to an interpretation of the Schottky anomaly in staurolite. No heat-capacity data exist for a diamagnetic phase isomorphous with staurolite. Furthermore, the approach used by Friedberg et al. (1962) assumes that all the paramagnetic ions experience the same zero-field splitting, that is, that all the paramagnetic ions reside in similar lattice sites having essentially identical crystal fields. Smith (1968) and Takéuchi et al. (1972) analyzed gamma-ray resonance spectra for staurolite and showed that the Fe site is only 77% occupied by Fe^{2+}. They have further shown that only 80% of the Fe^{2+} ions are located in the Fe sites. Similar results are given by Bancroft et al. (1967). The structure analysis of staurolite by Smith (1968) locates Fe^{2+} in the Fe site (tetrahedra) and in the Al(3A), Al(3B), U(1), and U(2) octahedra (using Smith's notation). The U(1) and U(2) octahedra are larger than the Al(3A) and Al(3B) octrahedra. Manganese is located in the U(1) and U(2) octahedra. Smith noted that the Fe^{3+} reported in chemical analyses of staurolites may represent oxidation during the analysis procedure because the Mössbauer pattern does not contain ferric iron peaks.

Assuming that the electric fields produced by the neighboring atoms at the Al(3A) and Al(3B) sites are essentially identical, and making similar assumptions for U(1) and U(2) and for the tetrahedral Fe sites, we conclude that the Fe^{2+} ions interact with a minimum of 3 different crystal fields which may yield a different distribution of split sublevels. This effect would not be seen in the results of Krupka, Hemingway, and Robie (1978, unpublished data) for enstatite because the crystal fields of the M_1 and M_2 sites would be nearly equivalent (Morimoto, 1959). Consequently, we would expect the maximum in the Schottky anomaly found by Krupka et al. (1978, unpublished data) and shown schematically in the model 2 data set to be more clearly defined and to represent a smaller energy spectrum than that seen in staurolite, as may be seen in Figure 2.

Some may ask, "If we know the approximate contribution of the iron group transition ions to the entropy, $R\ln(2S + 1)$, and, because at room temperature we are presumably at a temperature sufficiently greater than the maximum in the Schottky anomaly to assume that there is an equal distribution among the spin states and hence a constant magnetic contribution to the entropy, why do we worry about the specifics of the lattice and magnetic entropies at low temperatures?". The answer lies in the energetics of the system. Should a cooperative interaction exist, then the zero-splitting should be large compared to the exchange energy, and the specific heat of staurolite should exhibit a cooperative anomaly at a Néel point at some temperature less than the maximum in the Schottky anomaly, as was shown in the work of Friedberg et al. (1962) for $FeCl_2 \cdot 4H_2O$ (also see Kittel, 1976, Chapt. 14 and 15). Alternatively, should the magnetic contribution of the Fe^{2+} ion to the entropy of staurolite arise from a splitting of the magnetic sublevels into an upper triplet and lower doublet as is commonly seen in Fe^{2+} paramagnetic salts (Friedberg et al., 1962 and Lyon and Giauque, 1949), then a substantial contribution to the entropy could arise below 4 K from a splitting of the lower doublet. Without a reasonably valid model for the magnetic heat capacity distribution, we cannot determine what portion of the magnetic heat capacity has been measured directly with the calorimeter.

We may calculate the magnetic entropy for the iron transition group ions to be 44.1 J/mol · K or 43.2 J/mol · K if we assume all the iron as the Fe^{2+} ion based upon the corrected chemical analysis for the sample. The lattice entropy may be estimated in two ways, neither of which is very rigorous.

A first approximation to the lattice heat capacity may be obtained from a plot of $C_p T^2$ *vs.* T^5 following, for example, Friedberg et al. (1962). Using the roughly linear trend for the experimental data in the 20 to 30 K region, we obtain equation (1)

$$C_p = 5890T^{-2} + 81.25\times10^{-5}T^3 \qquad (1)$$

from which we estimate the lattice heat capacity as $C_L = 81.25\times10^{-5}T^3$. The heat capacity derived from this equation exceeds the measured heat capacity of staurolite above 35 K, and the calculated magnetic entropy (measured entropy less the estimated lattice entropy of 26.5 J/mol · K) is about half of that predicted from theory. The magnetic heat capacity approximation derived from equation (1) and designated as model 3 is shown graphically in Figure 3.

We are not surprised that the approach followed by Friedberg et al. (1962) fails for staurolite. The Schottky anomaly reported by Friedberg et al. was located at about 3 K where materials behave more like Debye solids than they do at the 20 to 30 K temperature range of the staurolite anomaly. Where multiple Schottky anomalies can be expected to be superimposed upon each other, as in the case of staurolite, a component of the lower temperature Schottky anomalies may contribute to the

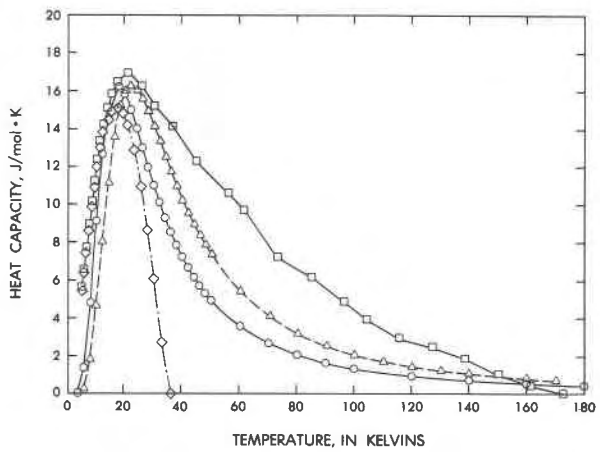

Fig. 3. Estimates of the magnetic heat capacity of staurolite. The diamonds represent the values obtained assuming the lattice heat capacity (model 3) obtained from equation (1). The open squares were obtained assuming the lattice heat capacity (model 2) obtained from equation (2). The triangles and circles were calculated from the equations of Lewis and Randall (1961), assuming an upper triplet and a lower doublet with a separation of 38.8 cm^{-1} and 30.7^{-1} respectively, as model 4.

slope derived from the data fit as C_pT^2 *vs.* T^5, causing an error in the estimate of the lattice component.

An alternate approximation to the lattice heat capacity may be made using the model 2 summation discussed above combined with the version of the corresponding-states argument presented by Lyon and Giauque (1949). Lyon and Giauque (1949) found the ratio of the heat capacity of $FeSO_4 \cdot 7H_2O$ to the heat capacity of diamagnetic $ZnSO_4 \cdot 7H_2O$, both taken at the same temperature, to vary linearly between 65 and 200 K. If we substitute the heat capacity of the synthetic $MgSiO_3$ (Krupka et al., 1978, unpublished data) for the calculated heat capacity of $FeSiO_3$ used in the model 2 approximation, then the scaled model 2 can be used as an estimate of the heat capacity of a diamagnetic phase for staurolite in the procedure described by Lyon and Giauque.

In Figure 4, we present a plot of the ratio of the heat capacity of staurolite, $C_{P,s}$ to the heat capacity of the scaled model 2 summation, $C_{P,2}$. Between 170 and 350 K, the ratio varies linearly. We can approximate the lattice heat capacity of staurolite from equation (2) if we assume that the model 2 summation is a reasonable approximation to the lattice heat capacity at room temperature and if we assume that the ratio maintains the same relationship at lower temperatures.

$$C_{P,s}/C_{P,2} = 1.000 + 3 \times 10^{-5}\,(T - 160.6) \qquad (2)$$

The construction of this model requires that the total thermal contribution to the excess heat capacity arising from the electronic system be fully developed below the temperature at which the ratio of $C_{p,s}/C_{p,2}$ becomes linear. The magnetic entropy calculated from this model at 170 K is 42.4 J/mol · K. This value represents about 96% of the theoretical magnetic entropy.

We present two additional estimates of the magnetic heat capacity of staurolite in Figure 3. In the first case, the lattice heat capacity estimates from equation (2) were subtracted from the observed heat capacity of staurolite. In the second case, following the procedures outlined by Friedberg et al. (1962), we may estimate the averaged separation of an assumed upper triplet of the ground state of the Fe^{2+} ion as 38.8 cm^{-1} from the coefficient of T^{-2} term in equation (1) and, following the equations given by Lewis and Randall (1961, p. 423), we calculate the magnetic entropy and heat capacity by assuming all iron as Fe^{2+}. For convenience, this shall be designated model 4. Also following Friedberg et al., one may calculate an average separation of 30.7 cm^{-1} from the temperature of the maximum in the Schottky anomaly.

Because of the complexity of the staurolite structure, we cannot expect to be able to extract physically meaningful data regarding the splitting of the ground state of the iron group transition ions in a particular site in staurolite from the measured heat capacity data, because the heat capacity is an average of all such effects. It is unlikely that either of the postulated energy levels is completely degenerate as we have assumed. However, Friedberg et al. (1962) have shown that, even though the number of levels and their distributions cannot be uniquely determined, one can eliminate some arrangements by examining the variation of the maximum of the Schottky anomaly, C_{max}, with the various arrangements of levels and distributions. Gopal (1966) presented a similar argument. For staurolite, we find that C_{max} from each approximation is close to the predicted $C_{max} = 0.62R$ for the model of energy levels used above.

Adequate measurements of paramagnetic resonance and susceptibility for staurolite have not been found in the literature. Runciman et al. (1973) have calculated a

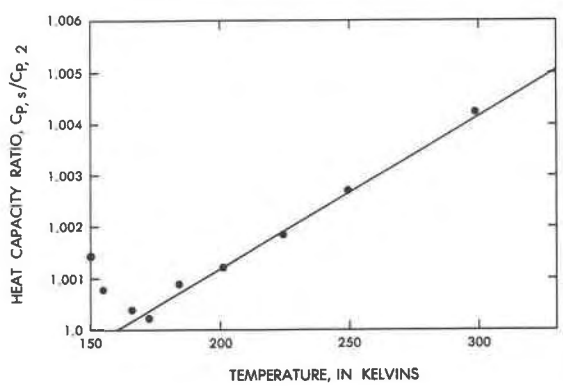

Fig. 4. Ratio of the measured heat capacity of staurolite to the heat capacity calculated at the same temperature from the modified version of the model 2 approximation discussed in text. The linear equation derived from this ratio is used to estimate the lattice heat capacity of staurolite below 100 K.

separation of 1.5 cm^{-1} for a lower doublet for Fe^{2+} in octahedral coordination in enstatite. They reported unpublished paramagnetic spectrum data in support of their interpretation. Similarly, Runciman et al. (1973) calculated a splitting of 0.27 cm^{-1} for Fe^{2+} in octahedral coordination in olivine. Friedberg et al. (1962) suggest a splitting of less than 0.8 cm^{-1} for the lower doublet for Fe^{2+} in octahedral coordination in $FeCl_2 \cdot 4H_2O$. Consequently, it is reasonable to assume that the crystal field of staurolite would cause a small separation of the lower doublet of the ground state of Fe^{2+}. Because our specific heat measurements for staurolite show a continuous decrease (within the limits of experimental accuracy) both in the absolute value and in the estimated magnetic contribution below 15 K, we can safely assume that if a split lower doublet exists, the separation must be less than 0.8 cm^{-1}.

If model 4 were a fair representation of the behavior of Fe^{2+} in staurolite, then an entropy contribution of $R\ln 2$ per mole of Fe^{2+} would be developed below 1 K. This entropy contribution would be added to the values calculated from the model 2 and 3 approaches, yielding 60.9 and 45.0 J/mol · K, respectively, for the magnetic entropy. The model 4 heat capacities are not a good representation of either the model 2 or 3 estimated heat capacities. Although the peak temperatures and maxima values as derived from the model 2 and 3 approximations are generally consistent with these values derived from model 4, the agreement in estimated heat-capacity values is particularly poor at temperatures below the maximum in the Schottky anomaly where the lattice heat capacity contributions become negligible. Even when a separation of 30.7 cm^{-1} (see discussion of model 3 above) is considered, the slope of the Schottky anomaly at temperatures below the maximum is not consistent with the theoretical values calculated from model 4 (see Fig. 3).

Although several explanations for the difference between the theoretical and experimental estimated curves could be presented, we think that the mismatch reflects the antiferromagnetic ordering observed by Scorzelli et al. (1976), Dickson and Smith (1976), and Regnard (1976). The lack of a pronounced anomaly in the low temperature heat capacity of staurolite is not inconsistent with this interpretation when one considers the concentration of chemical impurities and the non-ideal distribution of Fe^{2+} in natural staurolite, where both effects would contribute to a broadening of the peak associated with spin ordering. Regnard and Scorzelli et al. have noted that at 4.2 K the quadrupole interaction is of the same order of magnitude as that produced by magnetic interactions.

A calculation of the magnetic entropy of staurolite based upon the model 2 lattice approximation discussed above yields a value of about 42 J/mol · K at temperatures sufficiently larger than the temperature of the maximum in the Schottky anomaly to allow us to assume that the magnetic contribution is constant. Although no claims are made herein for the absolute accuracy of our lattice model, we think that the model is sufficiently accurate to suggest that the measured heat capacity of staurolite and the extrapolation of these data to 0 K underestimate the magnetic contribution to the entropy of staurolite. On the basis of the evidence and observations presented above, limits can be placed upon the error in the entropy of staurolite attributable to unresolved magnetic entropy below 5 K as 10 ± 10 J/mol · K.

Chemical site-configurational contributions to the entropy of staurolite

Ulbrich and Waldbaum (1976) have calculated the chemical site-configurational and the magnetic contributions to the entropy of staurolite. These calculations are based upon a simplification of the occupanices reported by Smith (1968). For a chemical composition for staurolite as $H_4Fe_4Al_{18}Si_8O_{48}$, Ulbrich and Waldbaum gave 53.5 J/(mol · K) for the magnetic entropy (therefore assuming all iron as Fe^{2+}) and 23.0 J/(mol · K) for the chemical site-configurational entropy.

Smith (1968) and Takéuchi et al. (1972) have shown that the formula for staurolite adopted by Ulbrich and Waldbaum (1976) is too idealized, as it requires nearly half the iron to be in the ferric state for electroneutrality, which is at variance with experimental results showing iron to be predominantly in the ferrous state. Náray-Szabó and Sasvári (1958) have given the formula $H_2Fe_4Al_{18}Si_8O_{48}$ for staurolite which requires all iron to be in the ferrous state for electrostatic balance. Smith noted that this formula conflicts with the water contents reported by Juurinen (1956). Takéuchi et al. reported a substantially lower water content for the staurolite they studied than that found by Juurinen, but they still require three hydrogens per 48 oxygens.

On the basis of an analysis of the location of hydrogen in staurolite and eight chemical analyses for staurolite, Takéuchi et al. (1972) have shown that the ideal staurolite should have between 2 and 4 hydrogens per 48 oxygens. Substantial substitutions of divalent Mg for Al and of Al for Si can lead to higher water contents in staurolite. Thus, we may take the two formulations of Takéuchi et al. cited above to represent the two limiting cases for ideal staurolite.

Smith (1968) has shown that Al and Fe are found in slightly higher concentrations in the Al(3A) sites as compared to Al(3B). The Al(3) octahedra cannot accommodate concurrent occupancy of an octahedral cation and hydrogen (Takéuchi et al., 1972). This limitation would imply a correspondingly higher occupancy of hydrogen in the Al(3B) octahedra (the P(1B) sites of Takéuchi et al.). Takéuchi et al. found nearly identical occupancy of hydrogen in the P(1B) and P(1A) sites (where P(1A) is located in the Al(3A) octahedra). Consequently, we may treat the Al(3) octahedra as being identical, without causing a significant error in our estimates of the chemical site-configurational contribution to the entropy of staurolite.

Following the procedures and assumptions outlined by

Ulbrich and Waldbaum (1976) and using the site occupancy data of Smith (1968) as a guide, we may estimate 34.6 and 121.0 J/(mol · K) for the chemical site-configurational entropy contribution for staurolite having the compositions $H_2Al_2Fe_4Al_{16}Si_8O_{48}$ and $(H_3Al_{1.15}Fe^{2+}_{0.60})$ $(Fe^{2+}_{2.07}Fe^{3+}_{0.54}Ti_{0.08}Mn_{0.02}Al_{1.19})$ $(Mg_{0.44}Al_{15.26})Si_8O_{48}$, respectively.

Entropy of staurolite

The entropy of staurolite may be calculated through a summation of the calorimetrically determined entropy, the chemical site-configurational entropy, and additional magnetic entropy not extracted through the measured heat capacities, or obtained through an analysis of reversed phase equilibrium data. Ultimately, equilibrium data must be used to evaluate the accuracy of our estimates of the additional magnetic and chemical site-configurational entropies.

Our best estimate of the entropy of staurolite as $(H_3Al_{1.15}Fe^{2+}_{0.60})$ $(Fe^{2+}_{2.07}Fe^{3+}_{0.54}Ti_{0.08}Mn_{0.02}Al_{1.19})$ $(Mg_{0.44}Al_{15.26})Si_8O_{48}$ at 298.15 K and 1 bar is 1101.0±12 J/(mol · K); for $H_2Al_2Fe_4Al_{16}Si_8O_{48}$ our best estimate is 1019.6±12 J/(mol · K). An additional 10 J has been added to the entropy of the natural staurolite composition on the basis of our analysis of the magnetic entropy. We think that the assumptions that have been made in calculating the entropy of the latter composition will yield a value that may be considered to represent the minimum entropy for this ideal staurolite.

Relatively few experimental phase equilibrium data involving staurolite exist in the literature (Richardson, 1966, 1968; Hoschek, 1967, 1969; and Ganguly, 1968, 1972; Rao and Johannes, 1979; Yardley, 1981; Pigage and Greenwood, 1982). Of those data, many reactions involve phases like almandine, chloritoid, and Fe-cordierite for which we have no good estimates of the entropy. The equilibrium data are not reversed for reactions involving staurolite and iron phases, like magnetite, for which good estimates of the entropy exist. Consequently, we are unable to further examine the accuracy of our estimates of the entropy of staurolite at this time.

Acknowledgments

James A. Woodhead provided the gehlenite sample from material he synthesized and characterized for his PhD dissertation. E-an Zen provided the staurolite sample and supervised Jane H. Hammarstrom who prepared and characterized the sample. A FORTRAN program used to calculate the Schottky thermal functions was kindly provided by Robert Chirico. We thank our U.S. Geological Survey colleagues, H. Tren Haselton and Susan W. Kieffer for their helpful comments.

References

Bancroft, G. M., Maddock, A. G. and Burns, R. G. (1967) Applications of the Mössbauer effect to silicate mineralogy-I. Iron silicates of known crystal structures. Geochimica et Cosmochimica Acta, 31, 2219–2246.

Dickinson, B. L. and Smith, G. (1976) Low-temperature optical absorption and Mössbauer spectra of staurolite and spinel. Canadian Mineralogist, 14, 206–215.

Friedberg, S. A., Cohen, A. F. and Schelleng J. H. (1962) The specific heat of $FeCl_2 \cdot 4H_2O$ between 1.15 and 20 K. Journal of the Physical Society of Japan, 17, 515–517.

Ganguly, J. (1968) Analysis of the stabilities of chloritoid and staurolite and some equilibria in the system FeO–Al_2O_3–SiO_2–H_2O–O_2. American Journal of Science, 266, 277–298.

Ganguly, J. (1972) Staurolite stability and related parageneses: Theory, experiments, and application. Journal of Petrology, 13, 335–365.

Gopal, E. S. R. (1966) Specific Heats at Low Temperatures. Plenum, New York.

Hemingway, B. S., Krupka, K. M. and Robie, R. A. (1981) Heat capacities of the alkali feldspars between 350 and 1000 K from differential scanning calorimetry, the thermodynamic functions of the alkali feldspars from 298.15 to 1400 K, and the reaction quartz + jadeite = analbite. American Mineralogist, 66, 1202–1215.

Hill, R. W. and Smith, P. L. (1953) The anomalous specific heat of ferrous ammonium sulphate. Physical Society of London, Proceedings A, 66, 228–232.

Hoschek, G. (1967) Untersuchungen zum stabilitätsbereich von chloritoid und staurolith. Contributions to Mineralogy and Petrology, 14, 123–162.

Hoschek, G. (1969) The stability of staurolite and chloritoid and their significance in metamorphism of pelitic rocks. Contributions to Mineralogy and Petrology, 22, 208–232.

Juurinen, A. (1956) Composition and properties of staurolite. Annals of the Academy of Science Fennical, Series A. III Geol., 47, 1–53.

Kittel, C. (1976) Introduction to Solid State Physics. John Wiley & Sons, Inc., New York.

Klotz, I. M. (1950) Chemical Thermodynamics. Prentice-Hall, Inc. Englewood Cliffs, New Jersey.

Krupka, K. M., Robie, R. A., and Hemingway, B. S. (1979) High-temperature heat capacities of corundum, periclase, anorthite, $CaAl_2Si_2O_8$ glass, muscovite, pyrophyllite, $KAlSi_3O_8$ glass, grossular, and $NaAlSi_3O_8$ glass. American Mineralogist, 64, 86–101.

Lewis, G. N., and Randall, M. (1961) Thermodynamics. Revised by Pitzer, K. S. and Brewer, L., McGraw-Hill Book Co., New York.

Lyon, D. N. and Giauque, W. F. (1949) Magnetism and the third law of thermodynamics. Magnetic properties of ferrous sulfate heptahydrate from 1 to 20 K. Heat capacity from 1 to 310 K. Journal of the American Chemical Society, 71, 1647–1656.

Morimoto, N. (1959) The structural relations among three polymorphs of $MgSiO_3$-enstatite, protoenstatite, and clinoenstatite. Carnegie Institution of Washington Year Book, 58, 197.

Náray-Szabó, I. and Sasvári, K. (1958) On the structure of staurolite, $HFe_2Al_9Si_4O_{24}$. Acta Crystallographica, 11, 862–865.

Osborne, D. W. and Westrum, E. F., Jr. (1953) The heat capacity of thorium dioxide from 10 to 305 K. The heat capacity anomalies in uranium dioxide and neptunium dioxide. Journal of Chemical Physics, 21, 1884.

Pankratz, L. B. and Kelley, K. K. (1964) High-temperature heat contents and entropies of akermanite, cordierite, gehlenite, and merwinite. U.S. Bureau of Mines Report of Investigations, 6555.

Pigage, L. C. and Greenwood, H. J. (1982) Internally consistent estimates of pressure and temperature: The staurolite problem. American Journal of Science, 282, 943–969.

Rao, B. B. and Johannes, W. (1979) Further data on the stability of staurolite + quartz and related assemblages. Neues Jahrbuch für Mineralogie Monatshefte, 437–447.

Raquet, C. A. and Friedberg, S. A. (1972) Heat capacity of $FeCl_2 \cdot 4H_2O$ between 0.4 and 5.3 K. Physical Review B, 6, 4301–4309.

Regnard, J. R. (1976) Mössbauer study of natural crystals of staurolite. Journal de Physique, Colloque C6, 37, 797–800.

Richardson, S. W. (1966) Staurolite, Carnegie Institute of Washington Year Book, 65, 248–252.

Richardson, S. W. (1968) Staurolite stability in a part of the system Fe–Al–Si–O–H. Journal of Petrology, 9, 467–488.

Robie, R. A. and Hemingway, B. S. (1972) Calorimeters for heat of solution and low-temperature heat capacity measurements. U.S. Geological Survey Professional Paper 755.

Robie, R. A., Hemingway, B. S. and Takei, H. (1982) Heat capacities and entropies of Mg_2SiO_4, Mn_2SiO_4, and Co_2SiO_4 between 5 and 380 K. American Mineralogist, 67, 470–482.

Robie, R. A. and Hemingway, B. S., and Wilson, W. H. (1976) The heat capacities of Calorimetry Conference copper and of muscovite $KAl_2(AlSi_3)O_{10}(OH)_2$, pyrophyllite $Al_2Si_4O_{10}(OH)_2$, and illite $K_3(Al_7Mg)$ $(Si_{14}Al_2)O_{40}(OH)_8$ between 15 and 375 K and their standard entropies at 298.15 K. U.S. Geological Survey Journal of Research, 4, 631–644.

Robie, R. A., Hemingway, B. S. and Wilson, W. H. (1978) Low-temperature heat capacities and entropies of feldspar glasses and of anorthite. American Mineralogist, 63, 109–123.

Roth, W. L. (1964) Magnetic properties of normal spinels with only A–A interactions. Journal de Physique, 25, 507–515.

Runciman, W. A., Sengupta, D. and Marshall, M. (1973) The polarized spectra of iron in silicates. I. Enstatite. American Mineralogist, 58, 444–450.

Runciman, W. A., Sengupta, D., and Gourley, J. T. (1973) The polarized spectra of iron in silicates. II. Olivine. American Mineralogist, 58, 451–456.

Schottky, W. (1922) The rotation of atomic axes in solids (with magnetic, thermal and chemical applications). Physikalische Zeitschrift, 23, 448–455.

Scorzelli, R. B., Baggio-Saitorvitch, E. and Danon, J. (1976) Mössbauer spectra and electron exchange in tourmaline and staurolite. Journal de Physique, Colloque C6, 37, 801–805.

Smith, J. V. (1968) The crystal structure of staurolite. American Mineralogist, 53, 1139–1155.

Stout, J. W. and Catalano, E. (1955) Heat capacity of zinc fluoride from 11 to 300 K. Thermodynamic functions of zinc fluoride. Entropy and heat capacity associated with the antiferromagnetic ordering of manganous fluoride, ferrous fluoride, cobaltous flouride, and nickelous fluoride. Journal of Chemical Physics, 23, 2013–2022.

Takéuchi, Y., Aikawa, N., and Yamamoto, T. (1972) The hydrogen locations and chemical compositions of staurolite. Zeitschrift für Kristallographie, 136, 1–22.

Ulbrich, H. H. and Waldbaum, D. R. (1976) Structural and other contributions to the third-law entropies of silicates. Geochimica et Cosmochimica Acta, 40, 1–24.

Weller, W. W. and Kelley, K. K. (1963) Low-temperature heat capacities and entropies at 298.15 K of akermanite, cordierite, gehlenite, and merwinite. U.S. Bureau of Mines Report of Investigations 6343.

Westrum, E. F., Jr. (1983) Lattice and Schottky contributions to the morphology of lanthanide heat capacities. Journal of Chemical Thermodynamics, 15, 305–325.

Westrum, E. F., Jr., Essene, E. J. and Perkins, D., III (1979) Thermophysical properties of the garnet grossular: $Ca_3Al_2Si_3O_{12}$. Journal of Chemical Thermodynamics, 11, 57–66.

Woodhead, J. A. (1977) The crystallographic and calorimetric effects of Al–Si distribution of the tetrahedral sites of melilite. Ph.D. dissertation, Princeton, University Microfilms, Ann Arbor, Michigan.

Yardley, B. W. D. (1981) A note of the composition and stability of Fe-staurolite. Neues Jahrbuch für Mineralogie Monatschefte, H3, 127–132.

Zen, E-an (1981) Metamorphic mineral assemblages of slightly calcic pelitic rocks in and around the Taconic allochthon, southwest Massachusetts and adjacent Connecticut and New York. U.S. Geological Survey Professional Paper 1113.

Manuscript received, March 3, 1983;
accepted for publication, October 3, 1983.